J. Great Lakes Res. 33:736–750
Internat. Assoc. Great Lakes Res., 2007

Satellite SAR Remote Sensing of Great Lakes Ice Cover, Part 2. Ice Classification and Mapping

George A. Leshkevich[1,*] and Son V. Nghiem[2]

[1]*National Oceanic and Atmospheric Administration*
Great Lakes Environmental Research Laboratory
2205 Commonwealth Boulevard
Ann Arbor, Michigan 48105

[2]*Jet Propulsion Laboratory*
California Institute of Technology
4800 Oak Grove Drive, MS 300-235
Pasadena, California 91109

ABSTRACT. *During the 1997 winter season, shipborne polarimetric backscatter measurements of Great Lakes (freshwater) ice types using the Jet Propulsion Laboratory C-band scatterometer, together with surface-based ice physical characterization measurements and environmental parameters, were acquired concurrently with Earth Resource Satellite 2 (ERS-2) and RADARSAT Synthetic Aperture Radar (SAR) data. This polarimetric data set, composed of over 20 variations of different ice types measured at incident angles from 0° to 60° for all polarizations, was processed to radar cross-section to establish a library of signatures (look-up table) for different ice types. The library is used in the computer classification of calibrated satellite SAR data. Computer analysis of ERS-2 and RADARSAT ScanSAR images of Great Lakes ice cover using a supervised classification technique indicates that different ice types in the ice cover can be identified and mapped, and that wind speed and direction can have an influence on the classification of water as ice based on single frequency, single polarization data. Once satellite SAR data are classified into ice types, the ice map provides important and necessary input for environmental protection and management, ice control and ice breaking operations, and ice forecasting and modeling efforts.*

INDEX WORDS: *Synthetic Aperture Radar (SAR), Great Lakes, ice, classification, mapping, RADARSAT, ERS-2, satellite, remote sensing.*

INTRODUCTION

In his recommendations for Great Lakes ice research, Marshall (1966) concludes that "studies are needed to classify Great Lakes ice types, their distribution and drift during the winter, and the subtle changes in albedo and imagery which mark the gradual disintegration of the ice and the imminent breakup." Early investigations by various researchers were conducted to classify and categorize ice types and features (Chase 1972, Bryan 1975), to map ice distribution (McMillan and Forsyth 1976, Leshkevich 1976), and to monitor and attempt to forecast ice movement with remotely sensed data (Strong 1973, McGinnis and Schneider 1978, Rumer *et al.* 1979, Schneider *et al.* 1981). Most of the early classification and mapping research on Great Lakes ice cover was done by visual interpretation of satellite and other remotely sensed data (Rondy 1971, Schertler *et al.* 1975, Wartha 1977). Owing to the size and extent of the Great Lakes and the variety of ice types found there during the winter, the timely and objective qualities in computer processing of satellite data make it well suited for such studies.

In the world's largest freshwater surface, covering an enormous area of 245,000 km^2 with a drainage basin extending 1,110 km north-south and 1,390 km east-west, ice cover is inherently a large-scale problem. The ice cover of the Great Lakes is a

*Corresponding author. E-mail: george.leshkevich@noaa.gov

strong climate indicator, and its seasonal change in surface cover has a profound impact on regional environment, ecology, economics, navigation, and public safety. Knowledge of the ice cover and its interannual variability is critical for the assessment and prediction of the impact of the Great Lakes environment on socio-economic conditions.

Great Lakes ice cover information, including spatial coverage, concentration, ice type, thickness, freezeup and breakup dates, and ice duration, is an important and necessary input for environmental protection and management, ice control and ice breaking operations, and ice forecasting and modeling efforts. The nature of the ice cover problem in large lakes and in extensive waterways demands the use of satellite SAR data to satisfy the required high spatial resolution and the large aerial coverage simultaneously. A major utility of synthetic aperture radar (SAR) is its high spatial resolution, which is appropriate to monitor ice navigation hazards in shipping lanes in lakes and rivers.

In this paper (Part 2), results of algorithm development for Great Lakes ice classification and mapping using satellite SAR data are described with a focus on the application of the measured backscatter library of C-band signatures from numerous ice types presented in the companion paper (Nghiem and Leshkevich 2007) to calibrated ERS-2 and RADARSAT-1 SAR data. The main goal of this work is to develop an automated or semi-automated method to classify and map Great Lakes ice cover using satellite SAR digital imagery.

BACKGROUND

Much of the satellite ice interpretation algorithm development in the Great Lakes region began during the Extension to the Navigation Season Demonstration Study conducted during the 1970s. However, many of the early studies were done by subjective interpretation of satellite and other remotely sensed data. Starting in the mid-1970s, a series of studies including field studies and computer digital image processing, explored techniques and algorithms to classify and map freshwater ice cover using LANDSAT and Advanced Very High Resolution Radiometer (AVHRR) optical data and later, ERS-1/2 and RADARSAT SAR data (Leshkevich 1985; Leshkevich *et al.* 1990, 1997, 2000; Nghiem *et al.* 1998).

During winter months, cloud cover and short daylight hours over the Great Lakes impair the use of satellite imagery from passive sensors operating in the visible, near infrared, and thermal infrared regions. Even the daily repeat coverage from the AVHRR aboard the National Oceanic and Atmospheric Administration (NOAA) series of weather satellites produces only a few images per week showing regions of the Great Lakes that are useful for operational monitoring during winter months.

Passive microwave data acquired by satellite radiometers, such as the Special Sensor Microwave Imager (SSM/I), lack the spatial resolution required for monitoring and detailed analysis of Great Lakes ice cover. Although airborne high-resolution SAR or Side Looking Airborne Radar (SLAR) are used by the U.S. Coast Guard, the Canadian Ice Center (Atmospheric Environment Service 1988) (currently known as the Canadian Ice Service) and others for operational ice mapping, they are limited in their spatial and temporal coverage, are costly to operate, and are dependent on weather conditions for flight safety. The all-weather, day-and-night sensing capabilities of SAR make it well suited to monitoring winter conditions in the Great Lakes region, provided that data analysis algorithms can be developed.

The launch of the first ERS (ERS-1) SAR in July 1991 marked the beginning of a wealth of satellite-borne SAR data that were available throughout the 1990s, and continues more recently with the launch of the Advanced SAR (ASAR) sensor on the Environmental Satellite (ENVISAT), the launch of PALSAR on ALOS, and the future launch of RADARSAT-2. The satellite SARs used in this study all operate at C-band (5.3 GHz frequency, 5.7 cm wavelength) and include the ERS-1, with a vertically polarized SAR, the ERS-2, launched in 1995, also with a vertically polarized SAR, and RADARSAT, an operational satellite launched in 1995, with a horizontally polarized SAR, provide an opportunity for algorithm development.

METHODS

Previous Studies

In the results of a 1993 study using airborne (helicopter) reconnaissance data as "ground truth," preliminary computer analysis of ERS-1 images of Great Lakes ice cover using a supervised classification (level slicing) technique (Lillesand and Kiefer 1979) indicated that there was enough dynamic range in the backscatter signal allowing different ice types in the ice cover to be identified and mapped (Leshkevich *et al.* 1995).

To assess the utility of RADARSAT SAR data

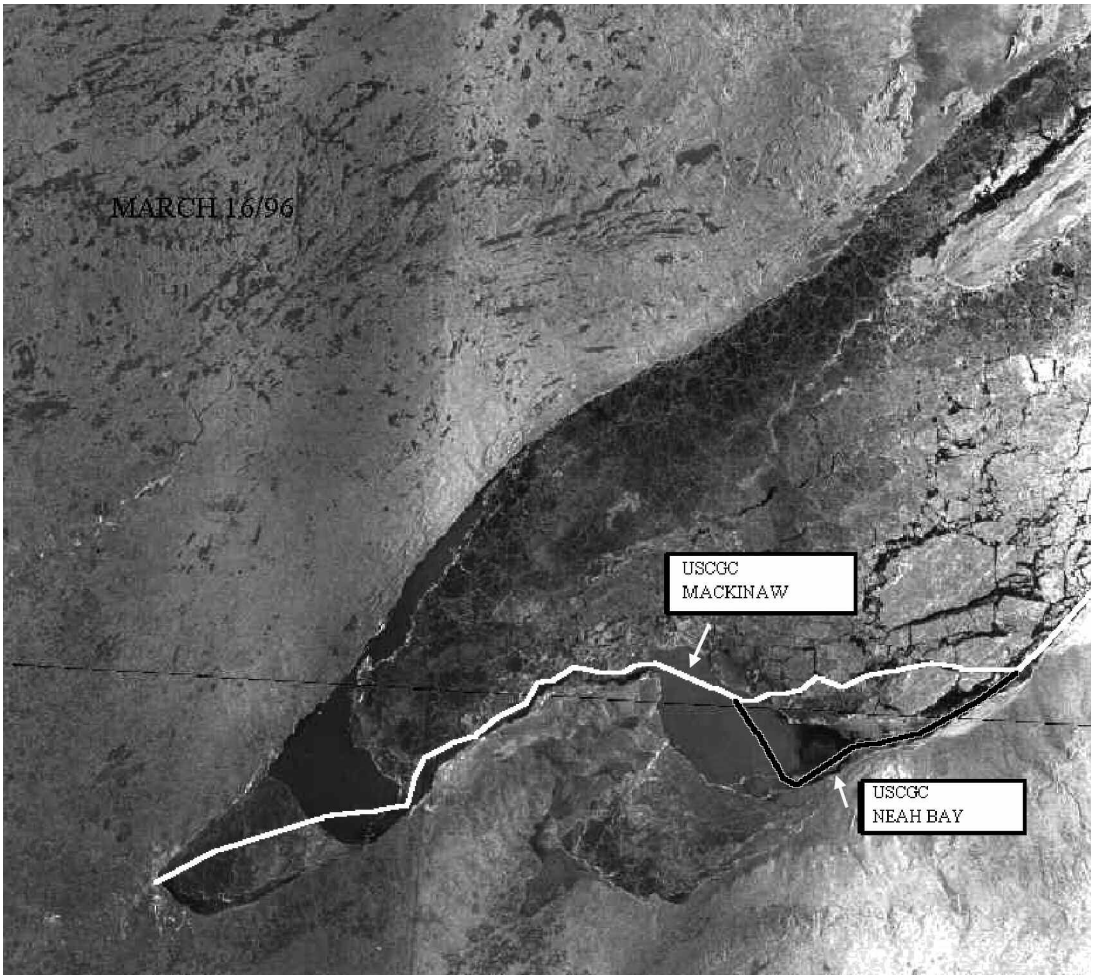

FIG. 1. RADARSAT ScanSAR Narrow Image (copyright RADARSAT International 1996), western Lake Superior, 16 March 1996.

for Great Lakes ice analysis, a data set for Lake Superior has been established covering the period from 13 to 21 March 1996. This data set includes RADARSAT ScanSAR data, AVHRR imagery, U.S. Coast Guard (USCG) SLAR, and surface (*in situ*) data consisting of ice charts, photographs, and video taken from the USCG Cutter (USCGC) *Mackinaw*, a Coast Guard ice breaker, and from a USCG helicopter. Meteorological data from selected ground stations are also included. Color photographs and video along with ice charts and Global Positioning System (GPS) data were obtained along the ship track and over the study areas from altitudes ranging from approximately 200 to 400 m. Ice thickness was obtained by measurements and visual examination enroute. RADARSAT SAR data from the Gatineau readout station in Canada were received at the National Ice Center (NIC) in Suitland, Maryland via a link between the U.S. and Canadian Ice Centers and forwarded to the Great Lakes Environmental Research Laboratory. Two ScanSAR Wide images having a nominal 100-m resolution and a ScanSAR Narrow image of western Lake Superior with a nominal 50-m resolution (Fig. 1) were used in this analysis.

A supervised (level slicing) classification, based on a comparison of digital values in the SAR scene representing known ice types as identified from the *in situ* data, was used in this initial analysis. Using photographs, ice charts, and field notes, two ice types (snow ice and new lake ice) and open water were identified in the computer-displayed SAR image, and a representative training set, consisting of a range of digital values, was extracted for each type. A color was assigned to each type (range of values) and then applied to the entire scene, produc-

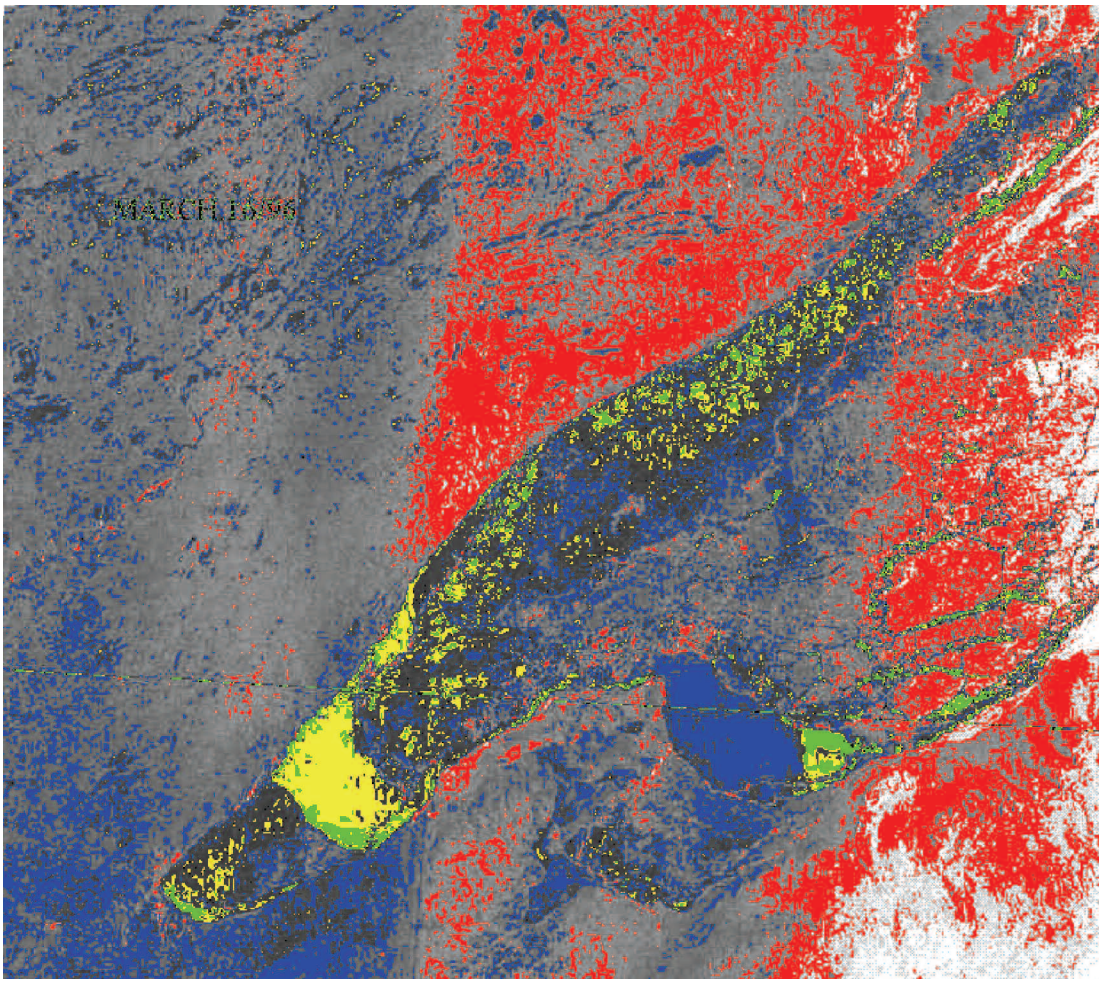

FIG. 2. Results of supervised (level slicing) classification of open water (blue) (yellow), new lake ice (green), and snow ice (red) in western Lake Superior, 16 March 1996.

ing a color-coded classified image. However, the ScanSAR Wide A (SWA) and Narrow data received from the Gatineau readout station were not calibrated and were "banded" or "striped," evidently due to an artifact in processing (mosaicing different antenna patterns). Calibration should greatly reduce this problem.

Although training sets were taken and processed within a "band," the results of the classification outside the band in which the training set was taken could be subject to error. For example, the training set for open water was selected in the "middle band" and color-coded blue. The training sets for new lake ice (green) and snow ice (red) were from the "right band." A training set for open water was also picked in the "left band" and color-coded yellow as the training set for open water picked in the "middle band" did not classify the open water in the "left band." This is probably largely due to the radiometric differences among the bands (mentioned above) as the areas are relatively close to each other and likely influenced by the same wind pattern. Figure 2 illustrates the results of the supervised (level slicing) classification of the western Lake Superior image (black, gray, and white are unclassified).

The 1997 Great Lakes Winter Experiment (GLAWEX'97)

To continue the development and validation of an algorithm for remote sensing of Great Lakes ice using SAR data, two winter experiments were conducted across the Straits of Mackinac and Lake Superior during February and March of the 1997

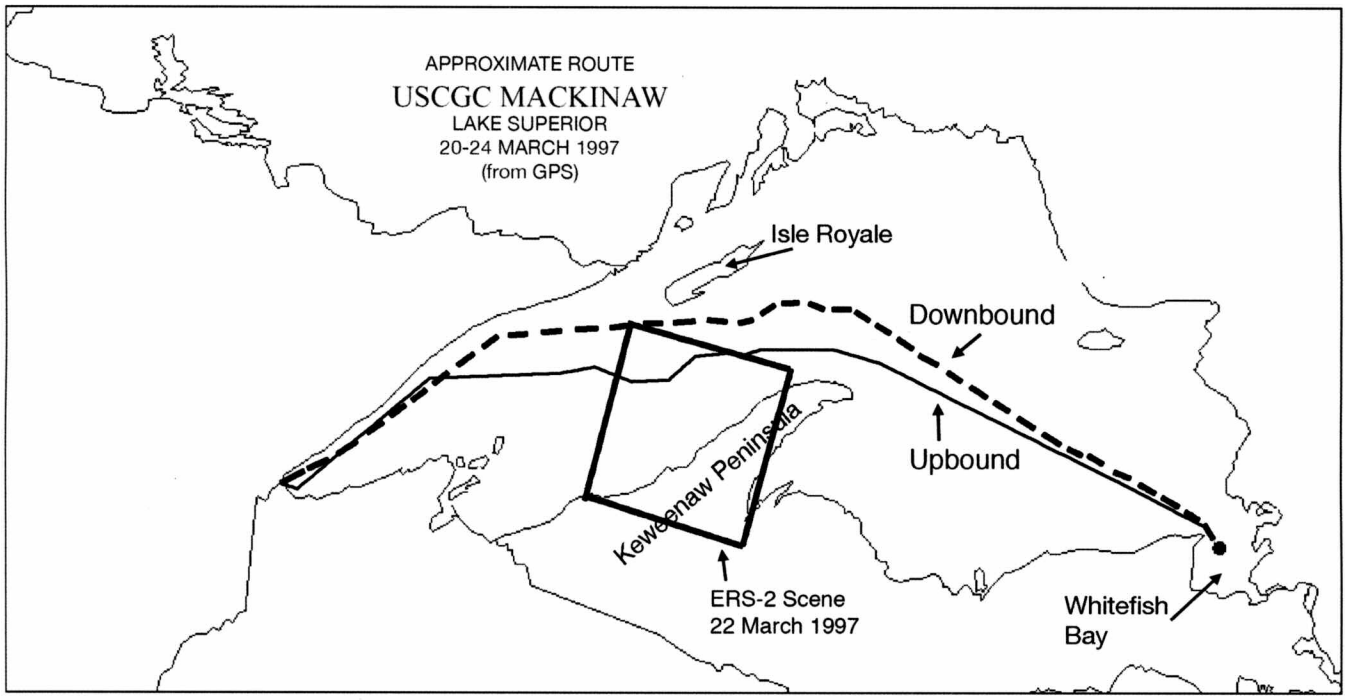

FIG. 3. Route of USCGC Mackinaw, Lake Superior, 20–24 March 1997. Box represents coverage of ERS-2 SAR scene, 22 March 1997.

winter season. The experiments acquired shipborne polarimetric backscatter data together with surface-based ice physical characterization measurements and environmental parameters in conjunction with aerial ice reconnaissance data. The experiments were timed to include RADARSAT-1 and ERS-2 SAR imaging.

In these experiments, the Jet Propulsion Laboratory (JPL) polarimetric scatterometer was mounted onboard the USCG ice breakers *Biscayne Bay* (February) and *Mackinaw* (March) (Nghiem and Leshkevich 2007). Figure 3 shows the route of the USCGC *Mackinaw* across Lake Superior in March, 1997. The scatterometer operates at C band and has full polarimetric capability (Nghiem 1993, Nghiem *et al.* 1997) including the horizontal (HH) and vertical (VV) co-polarizations and all other linear polarization combinations. Measurements were made at incident angles from 0° to 60° for each ice type so that the results are applicable to ERS-1/2 and RADARSAT SAR data, but can also be applied to other current and future satellite C-band SAR data. A video camera was used to observe lake ice types and surface conditions in the same direction of the scatterometer incidence at the same time and location of the backscatter measurements. Radar backscatter signatures of different ice types at different polarization, incidence angle, and temperature were processed to fully calibrated normalized radar cross-section (σ°) (Nghiem *et al.* 1998, Nghiem and Leshkevich 2007) to establish a library of signatures (look-up table) to be used in the computer classification of calibrated satellite SAR data.

Although backscatter measurements of different ice types with various snow cover, ice characteristics, and surface roughness were made at 20 different locations, ice and snow conditions at some locations were similar. Here we use backscatter signatures selected for different ice types commonly encountered over the Great Lakes. Although the ice naming convention starts with documented definitions (U.S. Dept. Commerce 1971, U.S. Navy Hydrographic Service 1952, Canadian Ice Service 2004), deviation from standard terminology was made in some cases to better describe the ice type in terms of stratigraphy, surface roughness, or other identifying characteristics as opposed to concentration. For example, a description like "patchy snow on snow ice over black ice" (along with a short name) was used to depict the ice types and layering or structure within the ice. In all cases, extensive areas of each ice type were measured and include:

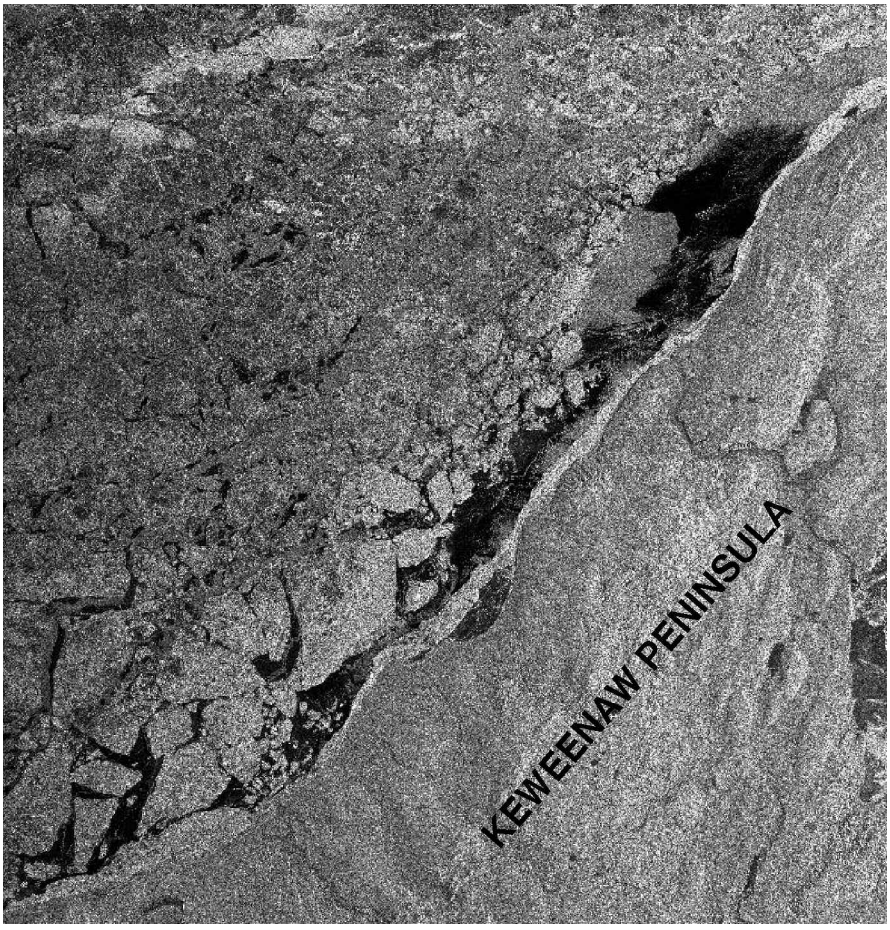

FIG. 4. ERS-2 image (Copyright ESA 1997) showing Lake Superior ice cover northwest of the Keweenaw Peninsula (lower right) on 22 March 1997.

(a) brash ice, (b) pancake ice, (c) patchy snow on snow ice over black ice (stratified ice), (d) older lake ice with patchy and rough snow cover (lake ice with crusted snow), (e) rough consolidated ice flows (consolidated ice floes), and (f) black ice with some snow dusting on surface (new lake ice). Photographs of the different ice types along with their physical characteristics are shown in Part 1 (Nghiem and Leshkevich 2007).

ERS-2

Initial Classification

ERS-2 SAR imagery was obtained and used in the initial study. A scene of the central portion of Lake Superior collected on 22 March 1997 (Fig. 4) was calibrated, and linear σ° values were converted to decibel (dB) according to the simplified equation for the derivation of σ° in Precision Image (PRI) products (Laur *et al.* 1997). Certain assumptions on the local incidence angle were made:

- A flat terrain is considered, i.e., there is no slope. The incidence angle depends only on the earth ellipsoid and varies from about 19.5° at near range to about 26.5° at far range .
- Any change in incidence angle across a distributed target is neglected, i.e., a distributed target corresponds to one average value of the incidence angle, thanks to the small range of ERS incidence angles (23° was used).

Measured backscatter values (in dB) for three non-overlapping ice types and calm water measured with the JPL C-band scatterometer on 21, 22, and

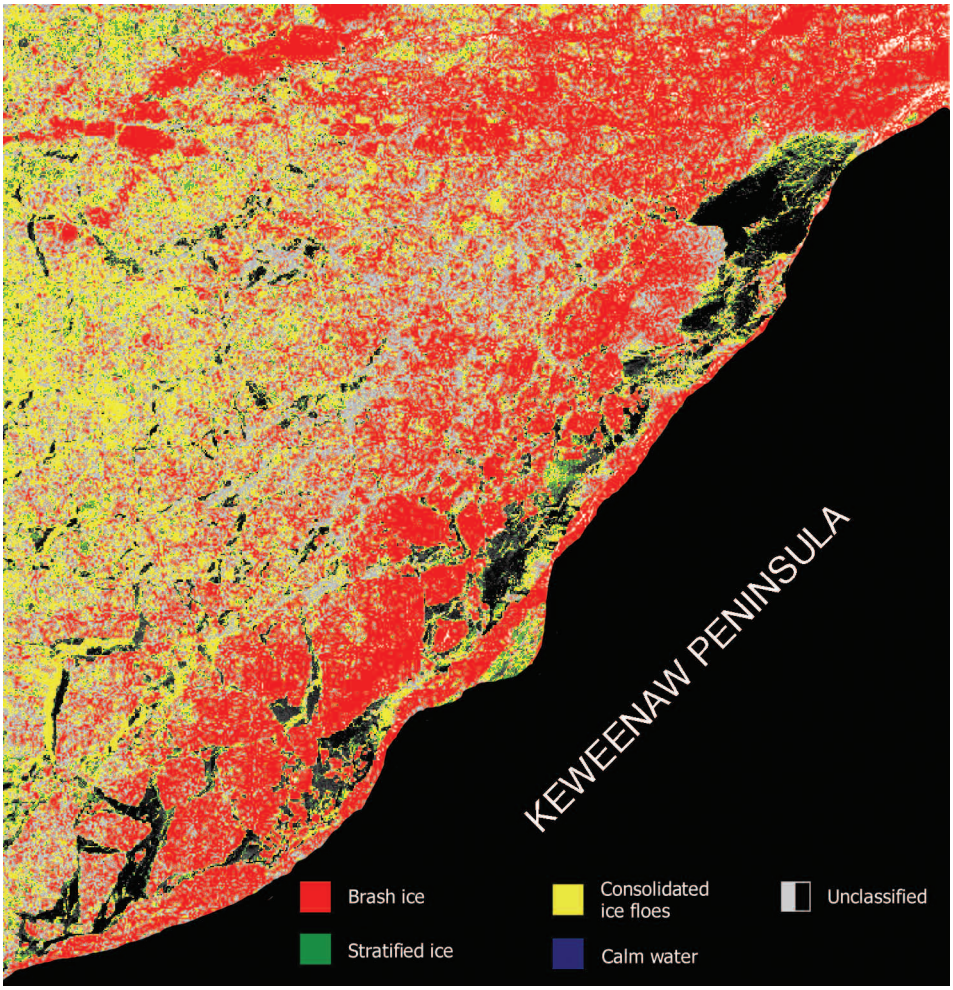

FIG. 5. Classified color-coded ERS-2 scene (22 March 1997) using measured backscatter values for consolidated ice floes (yellow), brash ice (red), stratified ice (green), and calm water (blue). No calm water classified in this scene.

23 March were used as test "training sets" to classify the scene. We assume that the values for 21 and 23 March did not change significantly from 22 March as there was no significant change in temperature or precipitation conditions. The assumption is verified as values measured on 23 March were very comparable to those of a similar ice type measured on 22 March.

The measured backscatter values for consolidated ice floes, brash ice, stratified ice, and calm open water (essentially non-overlapping) were applied to the 8×8 pixel averaged digital ERS-2 SAR image. The averaging not only reduced the speckle but also resulted in an image similar in resolution to RADARSAT ScanSAR Wide images. The overall uncertainty is about ± 1 dB due to the averaging and the incidence angle effect.

Figure 5 shows the color-coded result of the classification. Most of the ice cover in the scene was classified as consolidated ice floes (yellow) or brash ice (red). Areas classified as stratified ice (green) are scattered throughout the ice cover, but no calm open water was classified in the scene. This sample was measured on 23 March when we were out of the area covered by this scene. Black and gray represent unclassified areas.

Correction for Power Loss

For accurate derivation of geophysical parameters from the normalized radar cross section

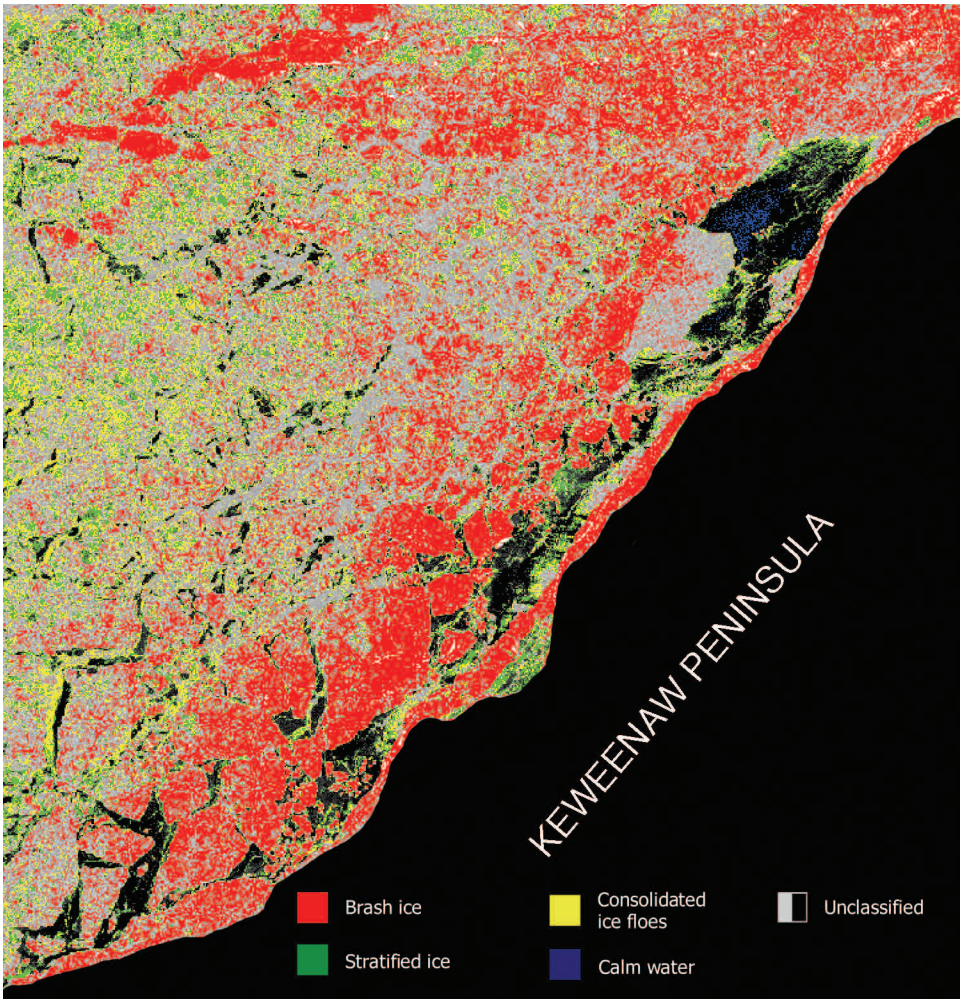

FIG. 6. Classified color-coded ERS-2 scene (corrected for power loss) using the same three ice types and calm water as in Figure 5, but accounting for local incidence angle effect. Calm water (blue) is classified in this scene.

(NRCS) of ERS-1 and ERS-2 SAR data, the NRCS has to be calibrated as accurately as possible. A problem with saturation within the analog-to-digital converter (ADC) of the ERS-1 and ERS-2 SARs leads to a power loss resulting in an underestimation of the NRCS. It has been determined that the highest power loss occurs over inland ice and in the near range of ocean surface images (Laur *et al.* 1997). To correct for power loss, the ERS-2 image (22 March 1997) was recalibrated as described in Rosenthal *et al.* (1998) using the programs *getit* and *calit* (Weinreich *et al.* 1998). In addition, to account for the effects of local incidence angle, the measured calibrated backscatter values for the three ice types and calm open water used as "training data" were interpolated every 0.5° between incident angles 19.5° and 26.5°. These "training data" sets were then used to classify the 8 × 8 pixel averaged recalibrated image.

Figure 6 shows the color-coded result of the classification of the image using the calibration algorithm for power loss and the correction for local incidence angle effect. As there were rather low power loss corrections to perform in this image, the results are similar to those described above. Two notable differences are that 1) there is more area classified as stratified ice (green), and 2) a small area of open water (blue) is classified in this image as the result of the more accurate calibration and "training data" sets.

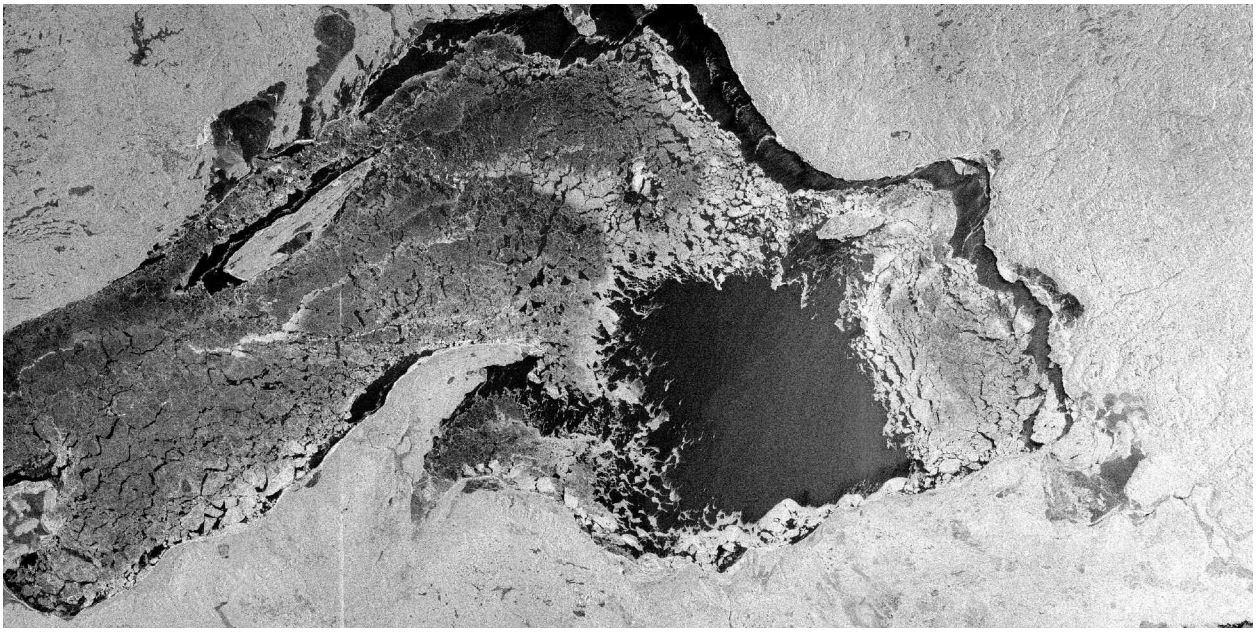

FIG. 7. RADARSAT-1 SWA (copyright RADARSAT International 1997) scene of Lake Superior ice cover on 22 March 1997.

Our route across Lake Superior passed through the northwest portion of the scene. The area of open water adjacent to the Keweenaw Peninsula appears reasonable. There is a strong current (Keweenaw Current) that flows along the deep nearshore area adjacent to the Keweenaw Peninsula that tends to keep the nearshore ice broken and moving. The classification can be improved by inclusion of additional ice types in the training data set. Although further validation needs to be done, this study demonstrates the capability of classifying Great Lakes ice types in calibrated satellite SAR imagery using backscatter values measured from different ice types as "training data."

RADARSAT

During the 1997 GLAWEX winter experiment, RADARSAT imagery was acquired over Lake Superior coincident with backscatter measurements on 22 March (Fig. 7), the same day as the ERS-2 image used in the initial analysis. Subsequent to the ERS-2 scene analysis, calibration techniques became available for RADARSAT-1 SWA from a number of sources including the Canadian Space Agency (CSA), as well as academic (Johns Hopkins University/Applied Physics Laboratory) and commercial (Satlantic, Inc.) institutions. The following two sections describe the results of ice classification of the RADARSAT scene using two different calibration techniques and classification methods. The RADARSAT results are compared to each other and to the classified ERS-2 scene.

JHU/APL Calibration

At the John Hopkins University/Applied Physics Laboratory (JHU/APL), algorithms have been developed to derive high resolution winds from RADARSAT ScanSAR data. For such purpose, the RADARSAT images need to be accurately calibrated. The data produced at the Gatineau receiving station are calibrated to beta naught (β°), but are also 2×2 block averaged at the Canadian Ice Service before being sent to the NIC. This block averaging complicates the calculation of incidence angles needed to derive sigma naught (σ°) values and has to be accounted for in the software. Using equations provided by the Canadian Space Agency/Radarsat International (RADARSAT International 1997), software was written at the JHU/APL (Monaldo 2005) to output an image calibrated to radar cross-section (σ°) from operational RADARSAT SWA data received by the U.S. National Ice Center (NIC) from the Canadian Ice Service via the North American ice link.

The 22 March RADARSAT scene was processed using the calibration software developed at

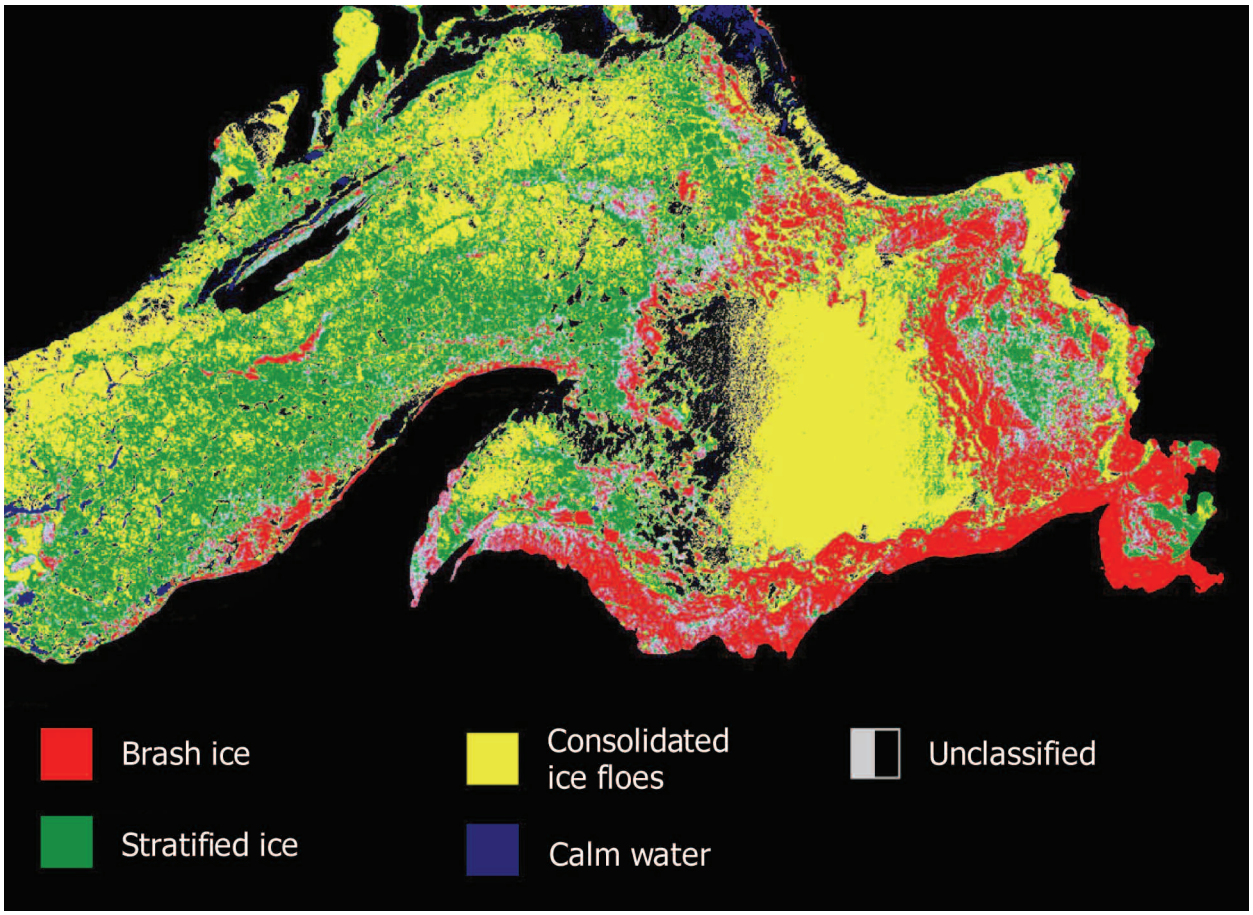

FIG. 8. Classified color-coded RADARSAT-1 scene (22 March 1997) calibrated to σ° using the JHU/APL software. Measured backscatter values for consolidated ice floes (yellow), brash ice (red), stratified ice (green), and calm water (blue) were used as training sets.

JHU/APL, producing a 4 × 4 block averaged image calibrated to σ° in dB. Using our library of calibrated C-band backscatter signatures (Nghiem and Leshkevich 2007) corresponding to the RADARSAT SWA HH polarization and incident angles, the scene was classified and color-coded using the same four essentially non-overlapping training sets and classification technique as was used for the ERS-2 scene. Figure 8 shows the results of the classification.

Satlantic Calibration

Satlantic, Inc. is a commercial company that supplies remote sensing instruments, processing software, and services to the remote sensing community. Their SAR processor called SentrySAR (Dragosevic and Plache 2000) was used to read the Level 0 data for the 22 March scene obtained from the Gatineau receiving station and produce CEOS Level 1, flat binary beta naught, and flat binary sigma naught products for the scene.

For classification of this scene, the entire library of ice types and open water described in Table 1 and Figure 6 in Part 1 (Nghiem and Leshkevich 2007) was used as training data, and the classification method was modified. Since the library of signatures can output σ° as a function of incidence angle, backscatter signatures of the different ice types and open water at every one-degree incidence angle interval were used as training data to classify the scene (which was subset in a 4 × 4 window to more nearly match the size of the JHU/APL calibrated scene) by incidence angle of each pixel. Since the signatures are incidence angle dependent,

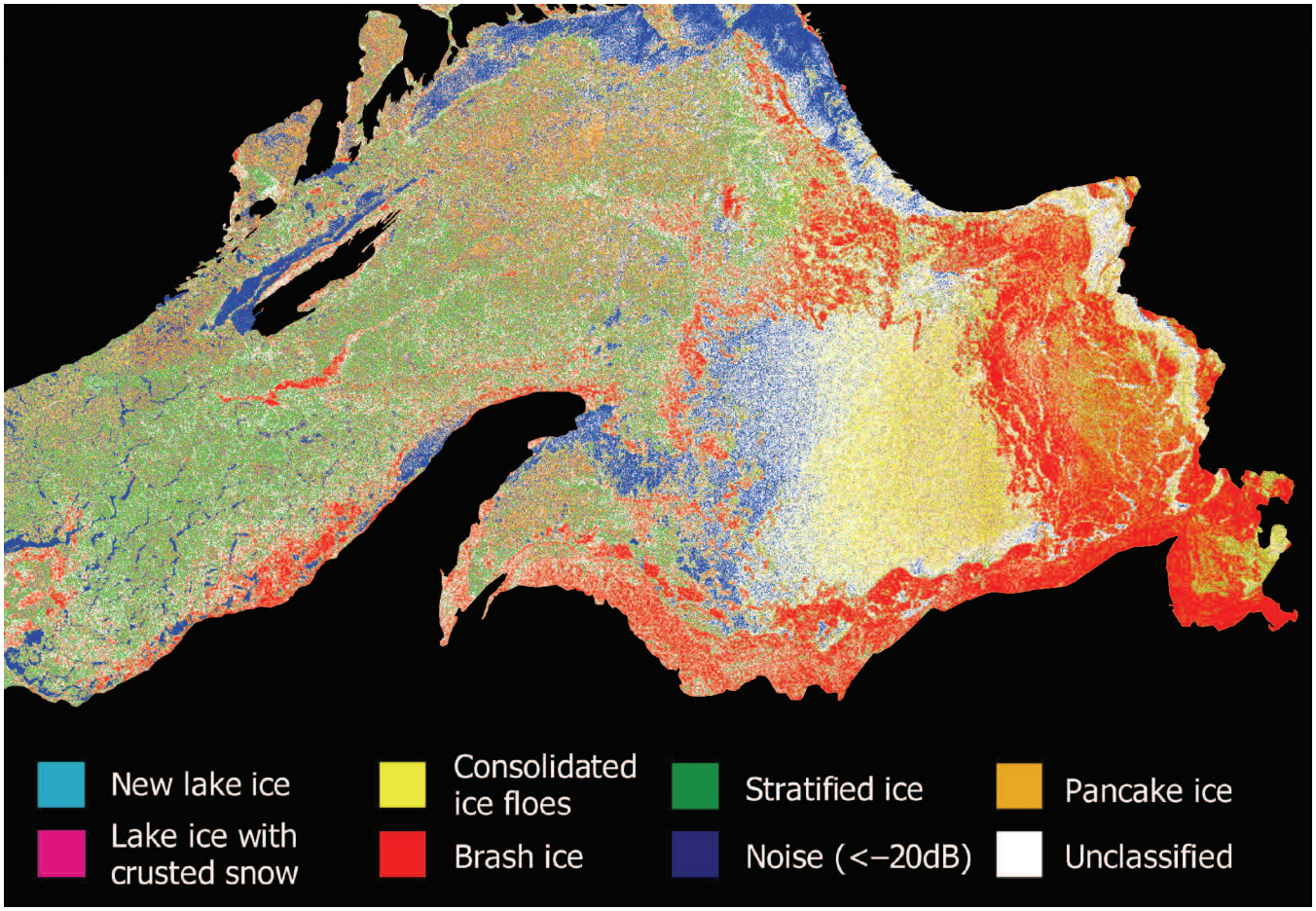

FIG. 9. Classified color-coded RADARSAT-1 scene (22 March 1997) calibrated to σ° by Satlantic, Inc. Measured backscatter values for consolidated ice floes (yellow), brash ice (red), stratified ice (green), new lake ice (cyan), lake ice with crusted snow (magenta), pancake ice (orange) were used as training sets. Areas below the RADARSAT noise floor (–20 dB) are coded blue and unclassified areas are coded white.

this should yield the most accurate classification results.

The incidence angle for each pixel in the scene was used to initiate a series of classification tests. First, the radar cross section of each pixel was compared to the minimum value of brash ice for the given incidence angle and, if greater than or equal to that value, the pixel was classified as brash ice. If not, the pixel was checked to see if it was less than or equal to the RADARSAT noise floor (–20 dB), which would account for types including calm water and new lake ice. If this test was not met, the radar cross section was matched against the minimum and maximum signature of each ice type in the library for the given incidence angle. If more than one ice type matched, the mean value closest to the radar cross section of the pixel determined to which ice type it was classified. The RADARSAT radiometric uncertainty is about ±1.0 dB in scene and ±1.5 dB in one orbit. However, since the overall uncertainty in calibration was estimated to be approximately ±2 dB including both RADARSAT and scatterometer radiometric uncertainty, the minimum and maximum signatures for each ice type were decreased and increased (respectively) by 2 dB to account for this uncertainty. The result is presented in Figure 9. In the next section, the results are compared to the classified JHU/APL and ERS-2 scenes.

RESULTS AND DISCUSSION

The objective is to show that our library of polarimetric C-band backscatter signatures can be applied to various sensor data calibrated using

TABLE 1. Summary of sensors, calibration source, and classification results

Satellite	Block average	Classification source	Number training sets	% overwater pixels classified
RADARSAT Figure 9	4×4 subset	SATLANTIC SentrySAR	7	73
RADARSAT Figure 8	4×4 of original 2×2	JHU/APL	4	78
ERS-2 Figure 6	8×8	ESA getit/calit	4	53

different software, and classified using different methods and can produce similar results. Because of differences in satellite sensors (different polarization and range of incidence angles), calibration schemes, pixel averaging, classification methods, and training data sets (Table 1), results for different images should not and cannot be compared on a one-to-one or pixel-to-pixel basis. As such, it is not our intention in this paper to endorse any one calibration method over any others.

The results show that similarities among the classified scenes are striking and outweigh the differences. The patterns of ice distribution are expectedly similar and the classification results reasonably similar. Differences can be attributed to one of several factors:

1) The library of signatures for all seven ice and water types, as well as a modified classification method, were used for the classification of the Satlantic scene, while four essentially non-overlapping types were used for the JHU/APL and ERS-2 scenes.
2) Different calibration methods were used for each of the scenes resulting in slightly different σ° products (values).
3) Although imaged on the same day, the ERS-2 and RADARSAT images were collected at different times, allowing time for ice movement in the more dynamic areas (such as along the Keweenaw Peninsula).
4) For the Satlantic classification, signatures less than –20 dB (RADARSAT noise floor) were color coded blue, which in the library of HH signatures would include calm open water and new lake (black) ice.
5) There are ice types in the scene that we did not get measurements of and are thus not in the library of signatures.

Despite these differences, the overall classification of ice types in each scene was very similar. For example, the strip of brash ice (red) located south of Isle Royale appears in all the scenes (Figs. 6, 8, 9), and the distribution of brash ice in Whitefish Bay and other areas of the lake are similar. The area along the west side of the Keweenaw Peninsula and color-coded blue (below RADARSAT noise floor) in the Satlantic calibrated scene (Fig. 9) was unclassified (black) in the JHU/APL calibrated scene (Fig. 8), although a few small areas along the northern shore and in the western parts of the scene were classified as open water (blue). In the ERS-2 re-calibrated scene, which has a lower noise floor than RADARSAT, open water is classified along the west side of the Keweenaw Peninsula. In addition, stratified ice (green) is the predominant ice type classified in the central and western portions of both the JHU/APL and Satlantic calibrated scenes (Figs. 8, 9) and also is a dominant type in the re-calibrated ERS-2 scene (Fig. 6) in the area west of the Keweenaw Peninsula.

One major difference is the extent of the area classified as consolidated ice floes (yellow) in the JHU/APL calibrated scene (Fig. 8). Although this type can be seen in the same areas (to the east and west of Isle Royale, for example) in the Satlantic calibrated scene (Fig. 9), it is not the dominant type but rather has pancake ice (orange), lake ice with crusted snow (magenta), and stratified ice (green) included. This may be an artifact of the level of pixel averaging in the JHU/APL calibrated scene. As can be seen in Figure 6 in Part 1 (Nghiem and Leshkevich 2007), this ice type (consolidated ice floes (yellow)) overlaps and can be mixed with others at all incidence angles. Another obvious misclassification (error of commission) in both the JHU/APL and Satlantic calibrated scenes (Figs. 8, 9) is the large area of open water in the east central

portion of the lake. This area of open water is classified as predominantly consolidated ice floes (yellow) in both scenes and is an example of the possible misclassification of one or more ice types with wind roughened water whose backscatter can cover a large range depending on wind speed, wind direction, and incidence angle. This is a major limitation of SAR operated at a single polarization in a single frequency band.

In conclusion, the measured library of signatures (both for HH and VV polarizations) appears to classify the majority of ice types in the ERS-2 re-calibrated scene and the RADARSAT scene collected on the same day, and the distribution and patterns of coverage are strikingly similar. Differences in the classification results between the JHU/APL and Satlantic calibrated RADARSAT scenes can be mainly attributed to differences in calibration, classification methodology, pixel averaging, and to the additional training data (ice types) used for the Satlantic classification, but also emphasize the need for an accurately calibrated scene as was documented by investigators for ocean wind retrieval (Vachon *et al.* 1999). Overall, classification by incidence angle (per pixel) is most accurate because the signatures are incidence angle dependent and this method best accounts for this variability. Unclassified areas in all scenes point to the need for additional types to be added to the library.

FUTURE ALGORITHM DEVELOPMENT

Advanced SARs on ENVISAT and the future RADARSAT-2 satellite have improvements in their measurement capabilities. For single-beam SAR modes in Imaging Swath number 1 (IS-1) to number 7 (IS-7) with incidence angles up to 45.3° (European Space Agency 2006), ENVISAT ASAR can measure backscatter with dual polarizations in co-polarized and/or cross-polarized modes. ENVISAT ScanSAR mode can be selected at either vertical or horizontal polarization; however, it is still limited to a single polarization. A preliminary analysis of ENVISAT ASAR Alternating Polarization (AP) images of Great Bear Lake in northern Canada indicates that the additional information contained in the co-polarized and cross-polarized data can help in the classification of different ice types in the ice cover and open water from ice under various wind conditions.

RADARSAT-2 SAR will have polarimetric capability in single-beam modes (Morena *et al.* 2004). Furthermore, RADARSAT-2 SAR has dual-polarization ScanSAR modes and a large range of incidence angles compared to ENVISAT SAR. In anticipation of these advanced SAR capabilities, the 1997 GLAWEX library was obtained with the JPL polarimetric C-band shipborne scatterometer for all polarization combinations and incidence angle up to 60°. Thus, this library will be applicable to both ENVISAT and RADARSAT-2 SAR data for Great Lakes ice classification and mapping.

During the 2002 GLAWEX field experiment campaign (Nghiem and Leshkevich 2003), polarimetric and inteferometric SAR data were collected at C band and L band using the JPL airborne SAR system (AIRSAR) coincident with in situ measurements across Lake Superior, upper Lake Michigan, and Lake Huron from the USCGC *Mackinaw*. This data set will be useful to develop new ice classification and mapping algorithms for C-band SARs such as ENVISAT and RADASAT-2, and L-band SAR such as the Advanced Land Observing Satellite (ALOS) Phased Array L-band Synthetic Aperture Radar (PALSAR) (Iragashi 2001) or the future L-band InSAR in the DESDynI Mission (National Research Council 2007).

ACKNOWLEDGMENTS

SAR data for this study were provided by the European Space Agency (ESA) and the Canadian Space Agency (CSA)/Radarsat International (RSI). The authors gratefully acknowledge individuals at the Ice Center Environment Canada and the U.S. National Ice Center for their efforts in obtaining and making available the RADARSAT and ERS-2 SAR imagery, to Dr. J. Horstmann of the GKSS Research Center (Germany) for his help in recalibrating the ERS-2 image to correct for power loss, to Dr. F.M. Monaldo of the Johns Hopkins University/Applied Physics Laboratory for use of his SAR calibration software and processing assistance and to Songzhi Liu (Cooperative Institute for Limnology and Ecosystems Research) for programming assistance. Our appreciation and thanks go to the U.S. Coast Guard, Ninth District for providing the ship, helicopter, and ground support essential to the success of this study. The research in this paper performed by Jet Propulsion Laboratory, California Institute of Technology, was sponsored by the National Oceanic and Atmospheric Administration (NOAA), through an agreement with the National Aeronautics and Space Administration (NASA). GLERL Contribution Number 1429.

REFERENCES

Atmospheric Environment Service. 1988. *Ice Services in Canada.* Ottawa: Environment Canada, Atmospheric Environment Service, Ice Branch.

Bryan, M.L. 1975. *A comparison of ERTS-1 and SLAR data for the study of surface water resources.* Final Report, ERIM No. 193300-59-F, prepared for the National Aeronautics and Space Administration by the Environmental Research Institute of Michigan, Ann Arbor, MI under Contract No. NAS5-21783.

Canadian Ice Service. 2004. *Lake Ice Climatic Atlas, Great Lakes, 1973–2002.* Ottawa, Ontario, Canada.

Chase, P.E. 1972. *Guide to ice interpretation: Satellite imagery and drift ice.* Final Report prepared for the U.S. Department of Commerce by The Bendix Corp, Aerospace Systems Division, Ann Arbor, MI, under Contract No. 2-35372.

Dragosevic, M., and Plache, B. 2000. Doppler tracker for a spaceborne ScanSAR system. *IEEE Transactions on Aerospace and Electronic Systems* 36(3):907–924.

European Space Agency. 2006. *Envisat ASAR Product Handbook, Issue 2.1.* ESA Publication.

Iragashi, T. 2001. ALOS mission requirement and sensor specification, *Advances in Space Res.* 28(1):127–131.

Laur, H., Bally, P., Meadows, P., Sanchez, J., Schaettler, B., and Lopinto, E. 1997. *Derivation of the Backscattering Coefficient σ° in ESA ERS PRI Products.* ERS SAR Calibration Doc. No. ES-TN-RS-PM-HL09, 2(4), European Space Agency, Frascati, Italy.

Leshkevich, G.A. 1976. Great Lakes ice cover, winter 1974–75, NOAA Technical Report ERL 370-GLERL 11. National Technical Information Service, Springfield, VA 22161, 42 pp.

_____ . 1985. Machine classification of freshwater ice types from Landsat-1 digital data using ice albedos as training sets. *Remote Sensing Environment* 17(3): 251–263.

_____ , Deering, D.W., Eck, T.F., and Ahmad, S.P. 1990. Diurnal patterns of the bi-directional reflectance of fresh-water ice. *Annals of Glaciology* 14:153–157.

_____ , Pichel, W., Clemente-Colon, P., Carey, R., and Hufford, G. 1995. Analysis of coastal ice using ERS-1 SAR data. *International Journal of Remote Sens*ing 16(17):3459–3479.

_____ , Nghiem, S.V., and Kwok, R. 1997. Satellite SAR Remote Sensing of Great Lakes Ice Cover Using RADARSAT Data. In *Proceedings, Fourth International Conference on Remote Sensing for Marine and Coastal Environments*, pp. I-126–134. ERIM. Orlando, FL, March 17–19, 1997.

_____ , Nghiem, S.V., and Kwok, R. 2000. Monitoring Great Lakes Ice Cover with Satellite Synthetic Aperture Radar (SAR). In *Proceedings, International Geoscience and Remote Sensing Symposium (IGARSS2000).* IEEE Geosecience and Remote Sensing Society. Honolulu, Hawaii, July 24–28, 2000.

Lillesand, T.M., and Kiefer, R.W. 1979. *Remote Sensing and Image Interpretation.* New York: John Wiley and Sons.

Marshall, E.W. 1966. *Air photo interpretation of Great Lakes ice features.* Great Lakes Research Division, Special Report No. 25, University of Michigan, Ann Arbor, MI.

McGinnis, D.F., and Schneider, S.R. 1978. Monitoring river ice breakup from space, *Photogrammetric Engineering & Remote Sensing* 44(1):57–68.

McMillan, M.C., and Forsyth, D.G. 1976. *Satellite images of Lake Erie ice, January–March 1975*, NOAA Technical Memorandum NESS-80, National Technical Information Service, Springfield, VA 22161.

Monaldo, F.M. 2005. *ANSWRS:APL/NOAA SAR Wind Retrieval System-Software Documentation Version 3.0.* Report: SRO-05-13. Johns Hopkins University/ Applied Physics Laboratory, Laurel, MD 20723-6099.

Morena, L.C., James, K.V., and Beck, J. 2004. An introduction to the RADARSAT-2 mission. *Canadian Journal of Remote Sensing* 30(3):22–234.

National Research Council. 2007. *Earth Science and Applications from Space: National Imperatives for the Next Decade and Beyond.* The National Academies Press, Washington, D.C.

Nghiem, S.V. 1993. C-band polarimetric scatterometer: System operation, sensitivity and calibration. *ONR Sea Ice Electromagnetics Workshop*, Hanover, NH, September 14–16, 1993.

_____ , and Leshkevich, G.A. 2003. *Great Lakes Winter Experiment 2002, Synthetic Aperture Radar Applications to Ice-Covered Lakes and Rivers.* Jet Propulsion Laboratory Document D-26226, California Inst. Tech., Pasadena, CA.

_____ , and Leshkevich, G.A. 2007. Satellite SAR remote sensing of Great Lakes ice cover, part 1. Ice backscatter signatures at C Band. *J. Great Lakes Res.* 33:722–735.

_____ , Kwok, R., Yueh, S.H., Gow, A.J., Perovich, D.K., Kong, J.A., and Hsu, C.C. 1997. Evolution in polarimetric signatures of thin saline ice under constant growth. *Radio Science* 32(1):127–151.

_____ , Leshkevich, G.A., and Kwok, R. 1998. C-Band Polarimetric Backscatter Observations of Great Lakes Ice. In *Proceedings, IEEE International Geoscience and Remote Sensing Symposium (IGARSS '98),* Seattle, WA, July 6–10, 1998.

Radarsat International. 1997. *RADARSAT Data Products Specifications.* Document Number RSI-GS-026, Version 2/0.

Rondy, D.R. 1971. *Great Lakes ice atlas.* NOAA Technical Memorandum NOS LSCR 1, National Technical Information Service, Springfield, VA, 22161.

Rosenthal, W., Horstmann, J., Lehner, S., Schulz-Stellenfleth, J., and Weinreich, I. 1998. *The Spatial Resolution of Marine Meteorological and Marine Biological Parameter Fields in Coastal Areas with ERS SAR.*

SARPAK Final Report. GKSS Research Center, Geesthacht, Germany.

Rumer, R.R., Crissman, R., and Wake, A. 1979. *Ice transport in Great Lakes.* Water Resources and Environmental Engineering Research Report No. 79-3 prepared for the Great Lakes Environmental Research Laboratory by the State University of New York at Buffalo, Department of Civil Engineering, and the Center for Cold Regions Engineering, Science and Technology, under Contract No. 03-78-B01-104.

Schertler, R.J., Mueller, R.A., Jirberg, R.J., Cooper, D.W., Heighway, J.E., Homes, A.D., Gedney, R.T., and Mark, H. 1975. *Great Lakes all-weather ice information system,* NASA Technical Memorandum NASA TM X-71815, National Technical Information Service, Springfield, VA, 22161.

Schneider, S.R., McGinnis, D.F., Jr., and Gatlin, J.A. 1981. *Use of NOAA/AVHRR visible and near-infrared data for land remote sensing.* NOAA Technical Report NESS-84, National Technical Information Service, Springfield, VA 22161.

Strong, A.E. 1973. New sensor on NOAA-2 satellite monitors during the 1972–73 Great Lakes ice season. In *Remote Sensing and Water Resources Management. Proceedings No. 17*, pp. 171–178. American Water Resources Association, Urbana, IL.

U.S. Department of Commerce. 1971. *Ice Glossary.* (HO 75-602). National Oceanic and Atmospheric Administration, National Ocean Survey, Lake Survey Center, Detroit, MI.

U.S. Navy Hydrographic Office. 1952. *A Functional Glossary of Ice Terminology.* (H.O. PUB. NO. 609), Washington, D.C.

Vachon, P.W., Wolfe, J., and Hawkins, R.K. 1999. In *The impact of Radarsat ScanSAR image quality on ocean wind retrieval.* In *Proceedings of CEOS Workshop,* Toulouse, France, October 26–29, 1999.

Wartha, J.H. 1977. *Lake Erie ice—winter 1975–76*. NOAA Technical Memorandum NESS-90. National Technical Information Service, Springfield, VA, 22161.

Weinreich, I., Lehner, S., and Knopfle, W. 1998. *Recalibration of ERS SAR images.* DLR/DFD Technical Report, ftp.dfd.dlr.de under *pub/geos_util*.

Submitted: 16 February 2007
Accepted: 20 June 2007
Editorial handling: William M. Schertzer